Journal of Solid State Chemistry 239 (2016) 159–164

Contents lists available at ScienceDirect

Journal of Solid State Chemistry

journal homepage: www.elsevier.com/locate/jssc

Layered vanadyl (IV) nitroprusside: Magnetic interaction through a network of hydrogen bonds

D.M. Gil [a,1], H. Osiry [b], F. Pomiro [c], E.L. Varetti [c], R.E. Carbonio [d,1], R.R. Alejandro [b], A. Ben Altabef [e,1], E. Reguera [b,*]

[a] Instituto de Química Física, Facultad de Bioquímica, Química y Farmacia, Universidad Nacional de Tucumán, San Lorenzo 456, T4000CAN San Miguel de Tucumán, Argentina
[b] Centro de Investigación en Ciencia Aplicada y Tecnología Avanzada, Unidad Legaria, Instituto Politécnico Nacional, México
[c] CEQUINOR (CONICET-UNLP), Facultad de Ciencias Exactas, Universidad Nacional de La Plata, 47 and 115, 1900, La Plata, Argentina
[d] INFIQC – CONICET, Departamento de Físico Química, Facultad de Ciencias Químicas, Universidad Nacional de Córdoba, Haya de la Torre esq, Medina Allende, Ciudad Universitaria, X5000HUA Córdoba, Argentina
[e] INQUINOA-UNT-CONICET, Instituto de Química Física, Facultad de Bioquímica, Química y Farmacia, Universidad Nacional de Tucumán, San Lorenzo 456, T4000CAN San Miguel de Tucumán, Argentina

ARTICLE INFO

Article history:
Received 3 December 2015
Received in revised form
26 February 2016
Accepted 18 April 2016
Available online 23 April 2016

Keywords:
Nitroprusside
Molecular magnetism
Hydrogen bonds
Layered solid
Vanadyl

ABSTRACT

The hydrogen bond and π-π stacking are two non-covalent interactions able to support cooperative magnetic ordering between paramagnetic centers. This contribution reports the crystal structure and related magnetic properties for $VO[Fe(CN)_5NO]\cdot 2H_2O$, which has a layered structure. This solid crystallizes with an orthorhombic unit cell, in the *Pna2₁* space group, with cell parameters **a**=14.1804(2), **b**=10.4935(1), **c**=7.1722(8) Å and four molecules per unit cell (Z=4). Its crystal structure was solved and refined from powder X-ray diffraction data. Neighboring layers remain linked through a network of hydrogen bonds involving a water molecule coordinated to the axial position for the V atom and the unbridged axial NO and CN ligands. An uncoordinated water molecule is found forming a triple bridge between these last two ligands and the coordinated water molecule. The magnetic measurements, recorded down to 2 K, shows a ferromagnetic interaction between V atoms located at neighboring layers, with a Curie-Weiss constant of 3.14 K. Such ferromagnetic behavior was interpreted as resulting from a superexchange interaction through the network of strong $OH\cdots O_{H2O}$, $OH\cdots N_{CN}$, and $OH\cdots O_{NO}$ hydrogen bonds that connects neighboring layers. The interaction within the layer must be of antiferromagnetic nature and it was detected close to 2 K.

1. Introduction

The magnetic interactions involving weak bonds such as π-π stacking or hydrogen bond are observed in coordination compounds with organic ligands, among them molecules with aromatic groups [1–3], but they are unusual for inorganic solids. These interactions are very important in various fields of research such as supramolecular chemistry, crystal engineering and spin-crossover materials. The magnetic ordering could be of ferromagnetic or antiferromagnetic nature, depending on the orbitals involved in the exchange or superexchange interaction between paramagnetic centers [4]. The long range magnetic ordering mediated by hydrogen bond, both ferromagnetic and antiferromagnetic, is observed in purely organic solids [5,6] and in coordination compounds involving paramagnetic metal centers and organic ligands [6,7]. Related with a low density of spin, the cooperative magnetic ordering through hydrogen bond in purely organic solids is only observed at very low temperature, usually below 2 K [5,6]. Certainly, the understanding on the mechanism involved in the exchange or superexchange integral through the hydrogen bond is even limited, nevertheless, abundant experimental evidence on its role in the magnetic properties of organic and coordination compounds is available [5–12]. In this contribution we are reporting the magnetic interaction between V(4+) ions located at neighboring layers of vanadyl nitroprusside dihydrate, $VO[Fe(CN)_5NO]\cdot 2H_2O$, through a network of hydrogen bond that connects the layers. To the best of our knowledge, this is the first example of a cyanide-based coordination compound with evidence of a superexchange interaction through a network of hydrogen bond.

Transition metal nitroprussides form a well-known series of

* Corresponding author.
E-mail address: edilso.reguera@gmail.com (E. Reguera).
[1] Members of the research career of CONICET.

http://dx.doi.org/10.1016/j.jssc.2016.04.025
0022-4596/

coordination compounds with potential applications in gases storage and separation [13–16], electrochemical devices [17] and for holographic information storage [18]. Their magnetic properties remain poorly documented [19,20] because they are usually obtained as 3D framework where the spin-bearing metal centers remain separated a distance of above 10 Å, with a weak super-exchange integral through the -N≡C-Fe(II)$_{LS}$-C≡N-chain. Such interaction is of antiferromagnetic nature and it is observed at very low temperature, usually below 5 K [21]. The interaction could be of ferromagnetic character through intercalated organic molecules in layered (2D) metal nitroprussides, which has been observed for 2D transition metal nitroprussides [21,22]. This contribution reports the preparation of 2D $VO[Fe(CN)_5NO]\cdot 2H_2O$, its crystal structure (solved and refined from powder X-ray diffraction data), and the related magnetic properties. The structural study was complemented with IR, Raman and UV–vis data.

2. Experimental

The material under study was prepared by mixing aqueous solutions of sodium nitroprusside, $Na_2[Fe(CN)_5NO]\cdot 2H_2O$ and vanadyl sulphate, $VOSO_4\cdot 5H_2O$. A blue precipitate appears after one week by slow evaporation of the solvent. The formed precipitate was aged within the mother liqueur for three days in the darkness and then separated by filtration and washed with distilled water. The synthesis of $VO[Fe(CN)_5NO]\cdot 2H_2O$ has been reported by reaction of aqueous solutions of $Ba[Fe(CN)_5NO]\cdot 2H_2O$ with $VOSO_4\cdot 5H_2O$ [23]. In this work, the precipitation of the complex was observed with the concentration of the solution. The nature of the resulting blue solid was established from laboratory PXRD, IR, Raman and UV–vis measurements.

The IR spectrum was recorded with a Pike ATR device and a Perkin spectrophotometer. The Raman spectrum of the solid was collected at RT in the 3500–50 cm^{-1} spectral range using a diode-pump solid state 532 nm green laser with 9.0 mW power at the sample for excitation in a Thermoscientific DXR microscope equipped with CCD detector. A confocal aperture of 50 μm slit was used and 80 expositions of 4 s were accumulated for the sample in order to achieve sufficient signal to noise ratio. UV–vis spectrum was collected with the integration sphere method. PXRD pattern for the solid $VO[Fe(CN)_5NO]\cdot 2H_2O$ was recorded at room temperature using a PANanalitycal X'Pert PRO diffractometer (40 kV, 40 mA) in Bragg-Brentano geometry with CuK_α radiation (λ = 1.5418 Å), between 5° and 100° in 2θ in steps of 0.02°. The unit cell parameters for $VO[Fe(CN)_5NO]\cdot 2H_2O$ were obtained running DICVOL program [24]. Le Bail method was used to decompose the diffraction patterns for single and overlapping intensities, using a pseudo Voigt function in order to describe the reflection peak shapes [25]. The crystal structure was solved ab initio by combination of few PXRD techniques. Heavy atom (Patterson) method for solving the structures was initially considered for finding the appropriate space group. Using SHELX program [26], the position for heavy atoms (V and Fe) was found. The remaining atomic positions of C and N from equatorial CN groups were found from Fourier difference method. The position of the axial NO, CN groups and water molecules were located in successive Fourier synthesis. The Rietveld method implemented in FullProf program was used for the crystal structure refinement [27]. During the refinement process, the Fe–C, C≡N and N=O interatomic distances were constrained to take values within the reported ranges for metal nitroprussides [27–30]. Details on the data collection and structure refinement for $VO[Fe(CN)_5NO]\cdot 2H_2O$ are available from Supplementary Information. The magnetic properties were studied recording the ZFC/FC curves in the 2–300 K range and the magnetization versus applied magnetic field using a SQUID MPMPS3 magnetometer (from Quantum Design). Both, DC and AC magnetic data were collected.

3. Results and discussion

3.1. IR, Raman and UV–vis spectra

Fig. 1 shows the IR spectrum for the title compound in the 4000–400 cm^{-1} spectral region. That figure includes the Raman spectrum in the region where the CN stretching bands appear (Inset). The IR and Raman bands with the corresponding assignment are listed in Supplementary Information. According to the IR and Raman spectra, the solid contains bridged and unbridged CN groups. This suggests that it crystallizes with a layered structure, where only the equatorial CN groups remain forming coordination bridges with the metal centers. For 2D metal nitroprussides, analogue CN stretching bands profile has been observed [21,22,29–31]. The broad band (an unresolved doublet) observed in the 3500 and 2500 cm^{-1} spectral range reveals the presence of a network of hydrogen bonds, probably involving water molecules and unbridged CN and NO ligands (discussed below). This is consistent with the appearance of two partially overlapped δ(H-O-H) bands of relatively high frequency, at 1644 and 1619 cm^{-1}, corresponding to hydrogen bonded and coordinated water molecules, respectively. The coordinated water molecule is probably found linked to the V(4+) ion of the vanadyl group, occupying the available axial coordination position for this metal in the supposed layered structure for the solid. The band located at 1950 cm^{-1} is assigned to the ν(NO) stretching vibration. This relatively high frequency value supposes a low electron density at the π^*(NO) orbital. The frequency of the ν(NO) vibration is highly sensitive to the interaction at the N end of the cyanide groups [32]. An increase for the electron subtraction at the N end induces a higher charge removal from iron atom via π*-back donation and this reduce the availability of electron density to populate the π^*(NO) orbital. The remaining bands observed in the IR spectrum (below 1000 cm^{-1}) located at 663, 640, 541, 475 and 422 cm^{-1}, were ascribed to vibrations within the nitroprusside ion, particularly to δ(FeNO), ν(FeN), $\delta(FeCN)_{eq.+ax}$, $\nu(FeC)_{eq,\ A'+A''}$ and $\nu(FeC)_{eq,A'}$ vibrations, respectively [33]. The medium intensity band that appears at 1100 cm^{-1} is assigned to the V=O stretching vibration.

The recorded UV–vis spectrum confirmed the nature of the formed solid as a nitroprusside salt of the vanadyl(4+) ion (see

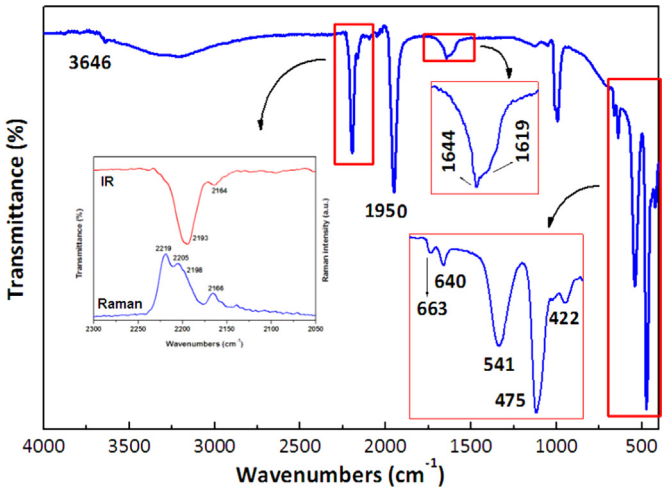

Fig. 1. IR spectrum for $VO[Fe(CN)_5NO]\cdot 2H_2O$. Inset (left): Comparison between IR and Raman spectra for the title compound in the 2300–2050 cm^{-1} region, where the CN stretching bands appear.

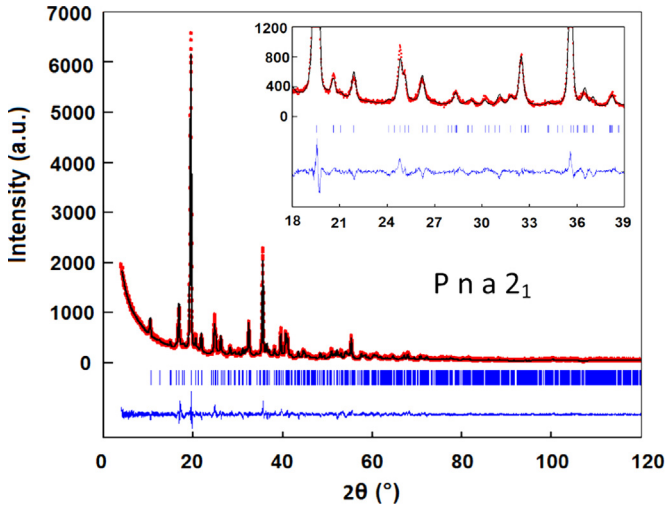

Fig. 2. Experimental, fitted and difference PXRD patterns for $VO[Fe(CN)_5NO]\cdot 2H_2O$. Inset: Zoom to illustrate the matching of the structural model to the experimental data.

Supplementary Information). The observed absorption bands in the spectrum correspond to metal-ligand electronic charge transfers within the nitroprusside anion. The bands observed at 318, 260 and 228 nm are assigned to $^1A_1 \rightarrow {}^1A_2$, $^1A_1 \rightarrow {}^1E$ and $^1A_1 \rightarrow {}^1E$ transitions, respectively [33,34]. The $^1A_1 \rightarrow {}^1A_2$ is essentially a d-d transition from the $2b_2$ orbital to $3b_1$ orbital. The band observed at 260 nm may be assigned to the orbitally allowed transition from 6e to $5a_1$ orbitals. The band located at 229 nm is ascribed to the transition from the 6e orbital to $3b_1$. In the title compound, vanadium is found with 4+oxidation state; with [Ar] $3d^1$ electronic structure. Most of oxovanadium complexes show three prominent bands in the electronic spectral region, which have been classified by Selbin as band I (909–625 nm), band II (667–556 nm) and band III (417–345 nm) [35]. According to Ballhausen et al. band I is assigned to $^2B_{2g} \rightarrow {}^2E_g$ transitions, band II as $^2B_{2g} \rightarrow {}^2B_g$ transition and band III is assigned to $^2B_{2g} \rightarrow {}^2A_g$ transition. In the spectrum of the title compound two bands located at 605 and 666 nm are observed, which are assigned to band II and band I, respectively. Band III is not always observed and being buried beneath a high intensity charge transfer band [35,36]. The pale blue color for the solid under study arises from absorption bands related to the mentioned d-d transitions.

3.2. Crystal structure

Fig. 2 shows the experimental, calculated and the difference PXRD patterns for the refined structural model of $VO[Fe(CN)_5NO]\cdot 2H_2O$ in the *Pna2₁* space group. A very good agreement between calculated and experimental profiles was observed (see Inset). All the attempts to obtain a reliable fitting within a centrosymmetric group failed (see Supplementary Information). This solid crystallizes within an orthorhombic unit cell with parameters **a**=14.1804 (2) Å, **b**=10.4935(1) Å, **c**=7.1722(8) Å. Four formula units are accommodated within the unit cell (Z=4). As expected, the Fe atom shows the pseudo octahedral coordination to five cyanide ligands and one nitrosyl group, which is characteristic of nitroprussides. The vanadium atom remains coordinated to four N ends of equatorial CN groups and its axial ligands are the oxygen atom of the vanadyl group and a coordinated water molecule (Supplementary Information). The recorded IR, Raman and UV–vis spectra (already discussed) support such structural model.

Fig. 3 shows the atomic packing within the unit cell for the refined crystal structure of the title compound. The refined atomic positions, occupation and thermal factors, and the calculated bond

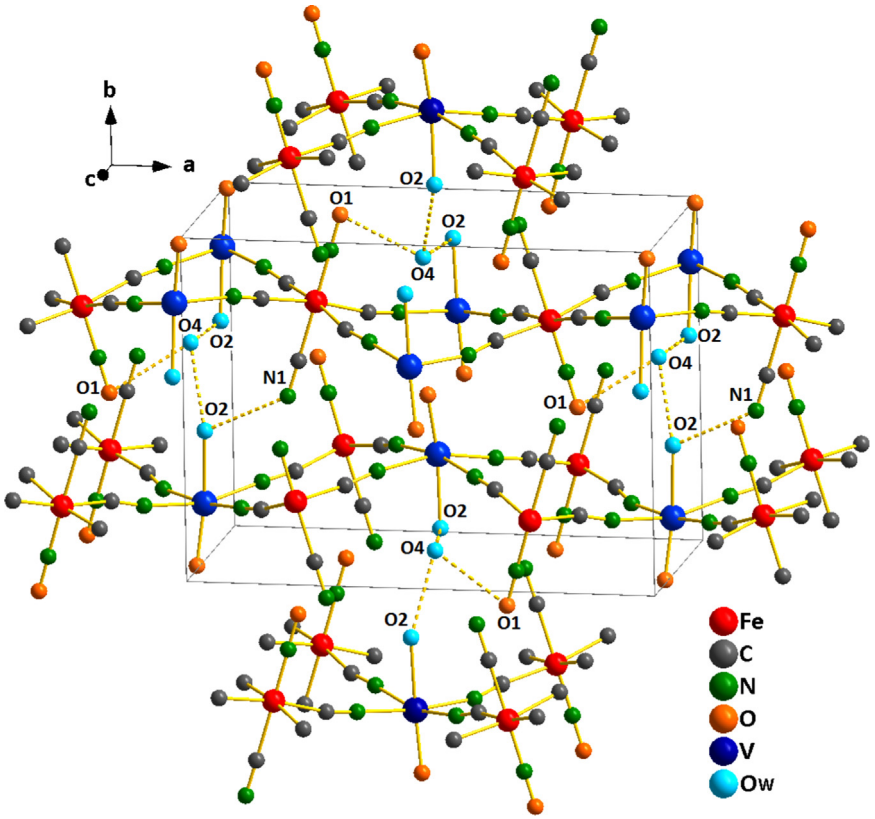

Fig. 3. Atomic packing within the unit cell for $VO[Fe(CN)_5NO]\cdot 2H_2O$. Neighboring layers remain linked through a network of hydrogen bridges involving the coordinated water molecules and unlinked CN and NO groups.

Table 1
Bond lengths (Å) and bond angles (°) for $VO[Fe(CN)_5NO]\cdot 2H_2O$.

Bond distances (Å)			
Fe–C1	1.927 (5)	V–N4^{iii}	2.153 (4)
Fe–C2	1.925 (5)	V–O2	1.885 (7)
Fe–C3	1.913 (6)	V–O3	2.241 (6)
Fe–C4	1.933 (6)	C1—N1	1.140 (6)
Fe–C5	1.905 (3)	C2—N2	1.141 (6)
Fe–N6	1.635 (3)	C3—N3	1.134 (6)
V–N1	2.123 (4)	C4—N4	1.133 (6)
V–N2^{i}	2.030 (4)	C5—N5	1.140 (4)
V–N3^{ii}	2.029 (4)	N6—O1	1.121 (4)
Bond angles (°)			
Fe–C1—N1	165.6 (5)	C5—Fe–N6	177.8 (3)
Fe–C2—N2	168.0 (5)	V–N1—C1	170.9 (5)
Fe–C3—N3	168.2 (5)	V–N2^{i}—C2^{i}	176.7 (5)
Fe–C4—N4	170.5 (5)	V–N3^{ii}—C3^{ii}	163.5 (5)
Fe–C5—N5	179.2 (16)	V–N4^{iii}—C4^{iii}	178.3 (5)
Fe–N6—O1	179.4 (8)	N1—V–N2^{i}	163.0 (4)
C1—Fe–C2	170.5 (4)	N1—V–N3^{ii}	84.6 (3)
C1—Fe–C3	92.8 (4)	N1—V–N4^{iii}	88.5 (3)
C1—Fe–C3	92.8 (4)	N1—V–O2	86.2 (3)
C1—Fe–C4	85.9 (4)	N1—V–O3	83.5 (3)
C1—Fe–C5	85.0 (4)	N2^{i}—V–N3^{ii}	95.8 (3)
C1—Fe–N6	93.0 (4)	N2^{i}—V–N4^{iii}	88.3 (3)
C2—Fe–C3	89.9 (4)	N2^{i}—V–O2	110.8 (3)
C2—Fe–C4	90.2 (3)	N2^{i}—V–O3	79.4 (3)
C2—Fe–C5	86.1 (4)	N3^{ii}—V–N4i^{ii}	168.8 (3)
C2—Fe–N6	95.9 (4)	N3^{ii}—V–O2	91.9 (3)
C3—Fe–C4	172.1 (2)	N3^{ii}—V–O3	91.0 (3)
C3—Fe–C5	87.5 (4)	N4i^{ii}—V–O2	96.3 (3)
C3—Fe–N6	93.3 (4)	N4^{iii}—V–O3	79.5 (3)
C4—Fe–C5	84.6 (4)	O2—V–O3	169.0 (3)
C4—Fe–N6	94.5 (3)		

Symmetry codes: (i) x+1/2, −y+1/2, z−1; (ii) x, y, z−1; (iii) x+1/2, −y+1/2, z.

Table 2
Hydrogen bond distances (Å) for $VO[Fe(CN)_5NO]\cdot 2H_2O$.

D–H···A	D···A
O3···O4	2.691 (4)
O3···O4^{iv}	2.689 (3)
O3···N5^{iv}	2.785 (4)
O1···O4^{iii}	2.834 (4)

Symmetry codes: (iii) x+1/2, −y+1/2, z; (iv) −x+1, −y, z+1/2.

distances and bond angles are available from Supplementary Information and were deposited in the ICSD database with the file number indicated below. The bond distances and bond angles are summarized in Table 1. For the vanadium atom, the coordination polyhedron is a distorted octahedron related to the nature of their mixed ligands, with axial metal-ligand distance from 1.885 (V-O_{VO}) to 2.241 Å (V-O_{H2O}). The equatorial metal-ligand distances are also different, from 2.029 to 2.153 Å. In accordance with evidence obtained from IR and Raman spectra, the solid under study crystallizes with a layered structure, where the axial NO and CN groups of the nitroprusside ion remain unbridged. Two types of water molecules were identified in the structure, one coordinated to the V(4+) ion and another hydrogen bonded to the first one. This last water molecule is found forming a triple bridge between coordinated water molecules from neighboring layers and an unbridged CN and NO ligands. Such network of hydrogen bonding interactions are connecting neighboring layers and support the material 3D framework. Table 2 contains the calculated donor-acceptor distances for the formed hydrogen bonds. These

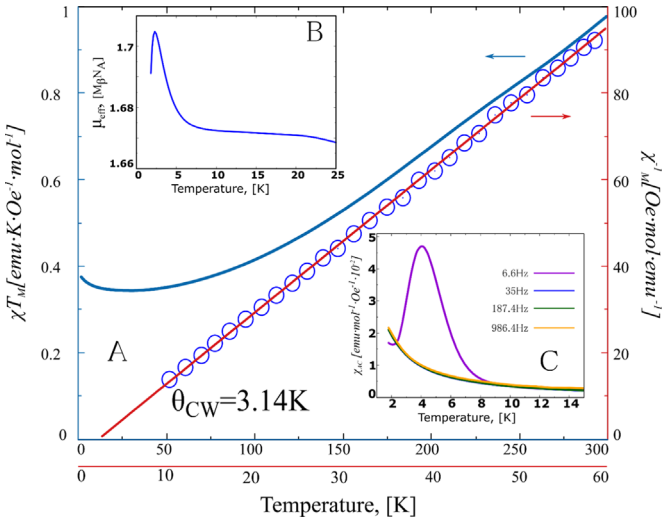

Fig. 4. χT versus T curve for $VO[Fe(CN)_5NO]\cdot 2H_2O$. Insets: (A) χ^{-1} versus temperature curve, below 60 K, used to estimate the Curie-Weiss temperature (θ_{CW}); (B) the temperature dependence for the effective magnetic moment (μ_{eff}); and (C) the AC susceptibility measured at different frequencies.

distances, in the 2.69–2.83 Å range, correspond to medium intensity hydrogen bonding interactions. The undulated configuration for the stacking of neighboring layers is consequence of that network of hydrogen bonds, and of the nature of the involved building units, the pseudo-octahedral metal coordination environments.

3.3. Magnetic properties

The iron (II) ion in the layered solid under study has a low spin configuration and, from this fact, it has a diamagnetic behavior. The V(4+) ion has a $3d^1$ electronic configuration which determines its paramagnetic character. Such paramagnetic centers are able to interact between them through the -N≡C-Fe-C≡N- chain and, at low temperature, a weak antiferromagnetic interaction could be observed. Such behavior has been detected for layered transition metal nitroprussides [21,22] and in 2D transition metals tetracyanonickelates [37–39]. Fig. 4 shows the χT versus T curve, which at low temperature shows certain deviation from a pure paramagnetic behavior. The Curie-Weiss constant (θ_{CW}), calculated from the inverse magnetic susceptibility (χ^{-1}) versus temperature curve is positive (3.14 K), with a fitting error no higher than 1.8 K. This suggests that at low temperature vanadium atoms from neighboring layers are involved in an incipient and weak ferromagnetic interaction (Fig. 4, Inset A). This is consistent with the observed features for the effective magnetic moment (μ_{eff}), calculated according to $\mu_{eff}=2.828\ \mathrm{sqrt}(\chi T)$[1]. On cooling, below 8 K a suddenly increase for the value of μ_{eff} was observed (Fig. 4, Inset B), which features a cooperative ferromagnetic type interaction. This is in accordance with the AC susceptibility, which shows a maximum at low frequency in that temperature region (Fig. 4, Inset C). At low frequency, the M(H) curve recorded by AC magnetometry, follows the result that would be obtained in the DC experiment. At high frequency, the AC signal disappears, which suggests that the imposed AC field is perturbing the weak magnetic interaction between neighboring V(4+) atoms through the network hydrogen bonds. Two possible ways are available for that interaction, through the hydrogen bonded water molecule, V-$O_{H2O}\cdots O_{H2O}\cdots O_{H2O}$-V, and through the unbridged CN and NO groups, V-$O_{H2O}\cdots N_{CN}$ and V-$O_{H2O}\cdots O_{NO}$. The interaction through the non-coordinated water molecule is of

medium intensity, with O-O distance of 2.69 Å (see Table 2) and it is probably responsible for the observed magnetic interaction. The vanadium atom has relatively extended d orbitals and this facilitates the overlapping with the p orbitals of the oxygen atom from the coordinated water molecule. The superexchange interaction supposes the presence of certain overlapping for the electronic clouds of coordinated and non-coordinated water molecules and this is possible by the existence of observed hydrogen bond between them. The V atom is found with a C_{2v} point group, with its unpaired electron probably located at d_{xy} orbital. The magnetic interaction could be of ferromagnetic nature because the unpaired electron resides in an orbital of π character while the V-$O_{H2O}\cdots O_{H2O}\cdots O_{H2O}$-V coupling involves a p orbital of the coordinated water molecules. The contribution from V-$O_{H2O}\cdots N_{CN}$ and V-$O_{H2O}\cdots O_{NO}$ is probably negligible because the pathway is unfavorable; it involves a larger distance between V centers. In order to shed light on the nature of the observed magnetic interaction, M(H) curves at different temperatures were recorded in order to construct Arrott plots [40]. No definite ferromagnetic long range ordering was identified in that plot at different temperatures (see Supplementary Information). That set of experimental evidence suggests the presence of an incipient interaction, of ferromagnetic nature, within a narrow temperature range, followed of a dominant antiferromagnetic ordering below 2 K. Below this temperature a pronounced decrease for the value of μ_{eff} is observed. This is consistent with the behavior observed for other transition metals 2D nitroprussides [21,22].

The recorded magnetization curve versus applied magnetic field recorded at 2 K is consistent with the above discussed evidence of an incipient ferromagnetic interaction between V(4+) atoms from neighboring layers. The maximum value of μ_{eff} is observed around that temperature. That curve corresponds to a weak but definite ferromagnetic ordering, with a definite hysteresis around zero applied field (Supplementary Information). Analogue ferromagnetic interaction between metal centers mediated by hydrogen bonds has been observed in 2D solids of natrochalcite-type, e. g. $Cu_2Na(H_3O_2)SO_4)_2$ [41]. The results herein discussed for a ferromagnetic type interaction between metal centers through a network of hydrogen bonds have no precedent within the series of transition metal nitroprussides.

4. Conclusions

The solid Vanadyl(IV) nitroprusside dihydrate, $VO[Fe(CN)_5NO]\cdot 2H_2O$ has been synthesized and characterized. The compound crystallizes with a layered structure, within an orthorhombic unit cell in the *Pna2₁* space group, with cell parameters **a**=14.1804(2) Å, **b**=10.4935(1) Å, **c**=7.1722(8) Å and Z=4 molecules per unit cell. The vanadium atom has a distorted coordination polyhedron formed by four equatorial N ends from CN groups with the axial positions occupied by the oxygen atom of the vanadyl group and a coordinated water molecule, corresponding to a C_{2v} point group symmetry around the V(4+) ion. An uncoordinated water molecule is found forming a hydrogen bond bridge between coordinated water molecules from neighboring layers. That uncoordinated water molecule forms an additional hydrogen bond with the axial CN ligand (or NO group). This water bridge between coordinated water molecules makes possible an incipient ferromagnetic coupling, through a superexchange interaction between vanadium ions located in neighboring layers. The unpaired electron in the V(4+) ion resides in the d_{xy} orbital while the superexchange interaction through the water molecules involves p orbitals of their oxygen atoms. Such orbitals are orthogonal and from this fact, the magnetic ordering must be of ferromagnetic character.

Supplementary information

Structural information derived from the crystal structure refinement is deposited and available from ICSD Fachinformationszentrum Karlsruhe (FIZ), (e-mail: crysdata@fiz-karlsruhe.de). CSD – number: 429,402, $VO[Fe(CN)_5NO]\cdot 2H_2O$.

Appendix A. Supplementary data

Experimental details, refined atomic positions, and occupation and thermal factors; experimental and fitted PXRD pattern and their difference, coordination geometry for the atoms involved in the material structure, and magnetization versus applied magnetic field curve.

Acknowledgements

This study was supported by CIUNT (Project D 0542/2). H. O. and E. R. thank the partial support from CONACyT (Mexico) through the projects 174247, 2013-05-231461, CB-2014-01-235840, and SRE-2013-191089. R. E. C. thanks support from CONICET PIP #11220120100360, ANPCyT PICT-2012-3079 and SECyT-UNC, Project 203/14. F. P. thanks CONICET for a doctoral fellowship.

Appendix A. Supporting information

Supplementary data associated with this article can be found in the online version at http://dx.doi.org/10.1016/j.jssc.2016.04.025.

References

[1] O. Kahn, Molecular Magnetism, VCH Publishers,, New York, 1993.
[2] N.A.G. Bandeira, D. Maynau, V. Robert, B.L. Guennic, Inorg. Chem. 52 (2013) 7980.
[3] L.-L. Li, K.-J. Lin, C.-J. Ho, C.-P. Sun, H.-D. Yang, Chem. Comm. 1286 (2006).
[4] K. Yoshizawa, R. Hoffman, J. Am. Chem. Soc. 117 (1995) 6921.
[5] A. Izuoka, M. Fukada, R. Kumai, M. Takura, S. Hikami, T. Sugawara, J. Am. Chem. Soc. 116 (1994) 2609.
[6] J. Cirujeda, M. Mas, E. Molins, F.L. de Panthou, J. Laugier, J.G. Park, C. Paulsen, P. Rey, C. Rovira, J. Veciana, J. Chem. Soc.: Chem. Commun. 709 (1995).
[7] J.S. Costa, N.A.G. Bandeira, B.L. Guennic, V. Robert, P. Gamez, G. Chastanet, L. Ortiz-Frade, L. Gasque, Inorg. Chem. 50 (2011) 5696.
[8] B.L. Guenic, N.B. Amor, D. Maynau, V. Robert, J. Chem. Theory Comput. 5 (2009) 1506.
[9] Y. Ma, A.-L. Cheng, E.-Q. Gao, Dalton Trans. 39 (2010) 3521.
[10] R.P. Doyle, M. Julve, F. Lloret, M. Nieuwenhuyzen, P.E. Kruger, Dalton Trans. 2081 (2006).
[11] M.S. Ray, A. Ghosh, S. Chaudhuri, M.G.B. Drew, J. Ribas, Eur. J. Inorg. Chem. 3110 (2004).
[12] K.R. O'Neal, T.V. Brinzari, J.B. Wright, C. Ma, S. Giri, J.A. Schlueter, Q. Wang, P. Jena, Z. Liu, J.L. Musfeldi, Scientific Reports 4, 1014, 6054.
[13] G. Boxhoorn, J. Moolhuysen, J.P.G. Coolegem, R.A. van Santen, J. Chem. Soc. , Chem. Commun. (1985) 1305.
[14] J. Balmaseda, E. Reguera, A. Gómez, J. Roque, C. Vazquez, M. Autie, J. Phys. Chem. B 107 (2003) 11360.
[15] J.T. Culp, C. Matranga, M. Smith, E.W. Bittner, B. Bockrath, J. Phys. Chem. B 110 (2006) 8325.
[16] L. Reguera, J. Balmaseda, C.P. Krap, E. Reguera, J. Phys. Chem. C. 112 (2008) 10490.
[17] M.H. Pournaghi-Azar, M. Hydarpour, H. Dastangoo, Anal. Chim. Acta 497 (2003) 133.
[18] V. Rusanov, S. Stankov, A.X. Trautwein, Hyperfine Interact. 144 (2002) 307 (and references therein).
[19] Z.-Z. Gu, O. Sato, T. Iyoda, K. Hashimoto, A. Fujishima, Chem. Mater. 9 (1997) 1092.
[20] M. Zentkova, M. Mihalik, I. Toth, Z. Mitroov, A. Zentko, M. Sendek, J. Kovac, M. Lukacova, M. Maryska, M. Miglierini, J. Magn. Magn. Mater. 272–276 (2004) e753.
[21] H. Osiry, A. Cano, A.A. Lemus-Santana, A. Rodríguez, R.E. Carbonio, E. Reguera,

J. Solid State. 230 (2015) 374.
[22] D.M. Gil, H. Osiry, A. Rodríguez, A.A. Lemus-Santana, R.E. Carbonio, E. Reguera, Eur. J. Inorg. Chem. 11 (2016) 1690–1696.
[23] E.J. Baran, S.B. Etcheverry, R.C. Mercader, Z. Anorg. Allg. Chem. 531 (1985) 199.
[24] A. Boultif, D. Louer, J. Appl. Cryst. 24 (1991) 987.
[25] A. Le Bail, H. Duroy, J.L. Fourquet, Mater. Res. Bull.. 23 (1988) 447.
[26] G.M. Sheldrick, Program for Crystal Structure Determination, Institute fur-Anorg. Chemie, GÖttingen, Germany, 1997.
[27] J. Rodríguez, Carvajal, Fullprof Suite 2013, Institute Leon Brillouin,, Sclay, 2013.
[28] D.F. Mullica, D.B. Tippin, E.L. Sappenfield, J. Coord. Chem. 25 (1992) 175 (and references therein).
[29] A. Gómez, J. Rodríguez-Hernández, E. Reguera, J. Chem. Cryst. 34 (2004) 893.
[30] H. Osiry, A. Cano, L. Reguera, A.A. Lemus-Santana, E. Reguera, J. Solid. State. 221 (2015) 79.
[31] A. Gómez, J. Rodríguez-Hernández, E. Reguera, J. Chem. Cryst. 34 (2004) 893.
[32] D.A. Estrin, L.M. Baraldo, L.D. Slep, B.C. Barja, J.A. Olabe, Inorg. Chem. 35 (1996) 3897.
[33] A. Benavante, J.A. de Morán, O.E. Piro, E.E. Castellano, P.J. Aymonino, J. Chem. Crystallogr. 27 (1997) 343.
[34] P.T. Manoharan, H.B. Gray, J. Am. Chem. Soc. 87 (1965) 3340.
[35] J. Selbin, Chem. Rev. 65 (1965) 153.
[36] C.J. Ballhausen, H.B. Grey, Inorg. Chem. 1 (1962) 111.
[37] M. González, A.A. Lemus-Santana, J. Rodríguez-Hernández, M. Knobel, E. Reguera, J. Solid State Chem. 197 (2013) 317.
[38] M. González, A.A. Lemus-Santana, J. Rodríguez-Hernández, C.I. Aguirre-Velez, M. Knobel, E. Reguera, J. Solid State Chem. 204 (2013) 128.
[39] F. Echevarría, A.A. Lemus-Santana, M. González, J. Rodríguez-Hernández, E. Reguera, Polyhedron 95 (2015) 75.
[40] A. Arrott, Phys. Rev. 108b (1958) 1394.
[41] S. Takeda, A. Watanabe, G. Maruta, T. Matsu, Mol. Cryst. Liq. Cryst. 376 (2002) 443.